V. QUANTUM ELECTRONICS

A. Laser Applications

Academic and Research Staff

Prof. Shaoul Ezekiel
Dr. Lloyd A. Hackel

Graduate Students

Michael B. Callaham
Kent H. Casleton
Robert E. Grove
Frederick Y-F. Wu

RESEARCH OBJECTIVES AND SUMMARY OF RESEARCH

Our interest is in the general area of precision measurements relating primarily to spectroscopy and the interaction of radiation with matter. Since many of the measurements that we perform require lasers with high spectral purity and excellent long-term stability, considerable effort is devoted to improving laser performance.

1. Long-Term Laser Frequency Stabilization Using a Molecular Beam

U.S. Air Force — Office of Scientific Research (Contract F44620-71-C-0051)

Shaoul Ezekiel, Lloyd A. Hackel

This research is motivated by a need for long-term stabilized lasers in the precision measurement of length. Such lasers would find application in earth-strain seismometry, optical communication, and fundamental measurements in experimental relativity and spectroscopy.

We are investigating the use of an I_2 molecular beam as a reference for the long-term frequency stabilization of an argon ion laser. A single-frequency argon ion laser operating at 5145 Å has been locked to an isolated hyperfine transition observed in a molecular beam of I_2^{127}. The long-term stability was measured by heterodyning the outputs of two independently stabilized lasers. A stability of several parts in 10^{14} has been achieved in an integration time of 300 seconds. The reproducibility of the laser frequency was investigated and preliminary results have demonstrated that the laser frequency can be reset within 7 parts in 10^{12}. Frequency shift caused by laser intensity variations was less than 8 parts in 10^{14} for a 1% change in intensity. External magnetic fields caused a shift of less than one part in 10^{14}/G.

2. Ultrahigh Resolution Spectroscopy Using Molecular Beams

U.S. Air Force — Office of Scientific Research (Contract F44620-71-C-0051)

Shaoul Ezekiel, Lloyd A. Hackel, Kent H. Casleton

The high spectral purity of well-controlled lasers makes it possible, in principle, to observe atomic and molecular spectra with extremely high resolution. Since Doppler

broadening is typically several hundred megahertz in the visible region, techniques for reducing Doppler and collisional broadening must be employed. The use of molecular beams is a convenient way of substantially reducing both Doppler and collisional broadening.

We have measured the complete hyperfine structure of the P(13) and R(15) (0-43) transitions in I_2^{127}, using laser-molecular-beam techniques with unprecedented precision. We have observed all of the 21 $\Delta F = \Delta J$(strong) components and 16 of the 18 $\Delta F = 0$(weak) components in the I_2 hyperfine structure. The frequency spacings of the lines were measured by heterodyning two argon lasers that are independently stabilized to different I_2 hfs components. The data were fitted with a standard deviation of 20 kHz to a theoretically calculated spectrum. We have included in the hfs Hamiltonian terms arising from nuclear electric quadrupole, spin-rotation, and spin-spin interactions. Further improvements in the measurement of frequency spacings may enable us to observe the effect of magnetic octopole interactions in I_2.

We have also investigated the line shapes of individual I_2 hfs lines with an instrumental resolution of one part in 10^{10}. The observed linewidth of 150 kHz (FWHM) which includes 75 kHz (FWHM) attributable to the natural width showed strong Lorentzian features.

JSEP

3. Single-Frequency Continuous-Wave Dye Laser

Joint Services Electronics Program (Contract DAAB07-74-C-0630)

Shaoul Ezekiel, Robert E. Grove, Frederick Y-F. Wu

The primary objective in this program is the development of an extremely stable, low-jitter, single-frequency cw dye laser for use in a variety of applications, as in optical communication and ultrahigh-resolution spectroscopy, and for studying fundamental interactions between radiation and matter.

During the past year, we have investigated the use of a freely flowing jet stream of Rhodamine 6G dissolved in ethylene glycol as a gain medium. The dye laser cavity is of the astigmatically compensated variety and single-frequency operation was accomplished with the aid of a Fox-Smith mode selector and two etalons. After a careful examination of the causes of laser jitter, we were successful in reducing the laser linewidth to less than 200 kHz. This narrow linewidth was demonstrated by a scanning Fabry-Perot interferometer with a 1-MHz instrument width. We used the tunable dye laser to excite extremely narrow resonances (700 kHz FWHM) in a molecular beam of I_2, which, as far as we know, is the highest resolution reported with a dye laser. Furthermore, we locked the dye laser to one of the hyperfine transitions in a molecular beam of I_2 and achieved a long-term stability of 6 parts in 10^{13} for an integration time of 25 seconds.

4. Single-Beam Reflection Holography

Joint Services Electronics Program (Contract DAAB07-74-C-0630)

Shaoul Ezekiel, Philip D. Henshaw, Antonio C. Pires

The aim of this program is to develop holographic nondestructive testing methods that are relatively simple to perform and do not require vibration isolation of the specimen.

JSEP

Our approach is based on the use of single-beam reflection holograms that can be

JSEP

reconstructed in white light. Such holograms can be made by clamping the hologram plate holder to the object under study so that little or no vibration isolation is needed.

During the past year, we have developed a technique for producing bright single-beam reflection holograms of simple objects. In this type of holographic arrangement, one single laser beam is passed through the hologram plate to provide the reference beam, as well as to illuminate the object on the other side of the plate. Light scattered by the object interferes with the laser beam incident on the photographic plate, thereby recording a hologram. Because of the geometry of this arrangement, interference fringes are recorded within the photographic emulsion so that the hologram may be viewed in white light by reflection. In addition to the convenience of white-light reconstruction (using a slide projector), this type of hologram requires very little vibration isolation. In fact, no isolation was used in our experiments.

The major drawback in single-beam reflection holography is that the object beam is necessarily much weaker than the reference beam, which results in a dim image. We have overcome this problem by the use of novel photographic processing techniques based on overexposure and underdevelopment, and have produced adequately bright holographic images.

We have used single-beam reflection holography for 3-D displays, as well as for double-exposure and time-average applications. We have also applied this technique to generate high-resolution (2.5 μm) surface depth contours on simple 3-D objects with white-light reconstruction.

JSEP

V. QUANTUM ELECTRONICS

B. Gaseous Lasers

Academic and Research Staff

Prof. William P. Allis
Prof. E. Victor George
Prof. Hermann A. Haus
Prof. Abraham Szöke
Dr. Paul W. Hoff
Dr. Charles K. Rhodes
Dr. Arthur H. M. Ross
Dr. Ehud Zamir
John J. McCarthy
William J. Mulligan

Graduate Students

John L. Miller
Charles W. Werner
David W. Wildman

RESEARCH OBJECTIVES AND SUMMARY OF RESEARCH

Our general objectives are concerned with a study of the plasma physics of gaseous lasers. We are continuing our studies on mechanisms that govern the rapid transfer of electrical energy into a high-pressure gas. One application of this study is the generation of high peak power laser pulses from a high-pressure (>10 atm) CO_2 laser system. We are devoting a major portion of our effort to obtain stimulated emission at ultraviolet frequencies from high-pressure noble gases.

JSEP

1. Ultraviolet Lasers

University of California, Livermore (Subcontract No. 7877409)
Joint Services Electronics Program (Contract DAAB07-74-C-0630)

E. Victor George

We have completed the kinetic modeling of the electron beam excited high-pressure xenon and krypton laser systems. Our modeling indicates that for the energy depositions encountered in many of these experiments ground-state absorption is not sufficient to explain the experimental results adequately. We have postulated that both the $^1\Sigma_u^+$ and $^3\Sigma_u^+$ states participate in the kinetic chain and that these states are collisionally coupled by interactions with electrons and heavy particles. That is,

$$M + X_2^*\left(^1\Sigma_u^+\right) \rightleftharpoons X_2^*\left(^3\Sigma_u^+\right) + M.$$

Here M represents either a heavy particle or an electron, and X_2^* either a xenon or krypton excimer. Preliminary results were presented at the Eighth International Quantum Electronics Conference in San Francisco, June 10-13, 1974, and have been published.[1] A more detailed paper on this work will be submitted for publication.

To facilitate our experimental program, we have acquired from the Lawrence Livermore Laboratory a 500 keV, 10 kA, 2 ns pulsed electron beam source (Febetron Model 706). The objective in this work is to measure experimentally some of the relevant and excited-state parameters and to compare these measurements with

JSEP

our theoretical predictions. Toward this end, we have developed a probe for measuring the time evolution of the electron density. This probe measures the reflection amplitude of an incident electromagnetic wave on the transient plasma in the time domain. Preliminary measurements indicate good agreement with theory. JSEP

In our effort to obtain stimulated vacuum ultraviolet emission from a conventionally excited high-pressure (pulsed) discharge, we have generated a constricted arc-free discharge at pressures up to 10 atm in xenon. We are making spectral vacuum ultraviolet measurements to determine the amount of 1700 Å emission by this plasma.

We shall begin soon an investigation into other potentially useful laser systems. This study will be restricted to high-energy density systems operating in the visible or ultraviolet regions of the spectrum.

2. CO_2 Laser

Joint Services Electronics Program (Contract DAAB07-74-C-0630)

E. Victor George

Our computer modeling of the high-pressure CO_2 laser system has indicated that a transmission-line energy transfer circuit is more efficient in terms of energy conversion than our previous lumped-element device. A redesign, including improved preionization, has been accomplished. Now we can operate routinely at 14.6 atm pressure (the present safety limit of our gas-handling equipment) and operation to ~20 atm should be possible. At 10 atm we obtain 200 mJ, 80 ns laser pulses on 5 rotational transitions. Detailed gain measurements have been made for the pressure range 2-14.6 atm. Comparisons of experimental results and theoretical predictions appear to be quite good. We are preparing a paper on this work for publication.

In our studies devoted to measuring the temporal characteristics of the electron density and understanding the role of ultraviolet preionization in atmospheric pressure CO_2 laser discharges, we have made transient high-pressure probe measurements on an ultraviolet preionized discharge. The measurements indicate that for gas mixtures typical of these devices (CO_2, N_2, He, and, in some instances, gas additives) the resulting plasma is attachment-dominated. The measured plasma loss rates have been used in the computer modeling. In our preionization studies (with the sustainer field absent) probe measurements have been correlated with preionizer source brightness, spectral content, time history, and so forth. Preliminary results indicate that vacuum ultraviolet emission single-step ionization is more important than, say, two-step processes.

References

1. C. W. Werner, E. V. George, P. W. Hoff, and C. K. Rhodes, "Dynamic Model of High-Pressure Rare-Gas Excimer Lasers," Appl. Phys. Letters 25, 235-238 (1974).

JSEP

JSEP

1. THEORETICAL PREDICTION OF CAPILLARY TUBE AMPLIFIER GAIN

Joint Services Electronics Program (Contract DAAB07-74-C-0630)
U.S. Army Research Office – Durham (Contract DAHC04-72-C-0044)

John C. AuYeung, Hermann A. Haus

Introduction

We have been studying the anomalously high gain of the flowing capillary CO_2 laser amplifier that had been reported by T. J. Bridges et al.[1] Our theoretical prediction of the gain is based on a model proposed by W. P. Allis and H. A. Haus[2] in which analytical expressions of the single-pass small-signal gain were obtained. We have found that the large gain achieved by Bridges et al. is due to a high electronic pumping rate made possible by a more effective cooling mechanism. The cooling was found to be better than conventional cooling in two respects. First, the beryllium oxide tube used in their experiments had an almost zero temperature gradient across the tube wall. Second, the gas-changing rate was so large that the flow was turbulent in nature, with a much more effective transverse heat-transfer mechanism. The effective thermal conductivity may be twice the value under laminar flow conditions.

Burkhardt, Bridges, and Smith[1] reported that by using a BeO tube, 1 mm bore, 10.2 cm long, with a mixture of CO_2-N_2-He of optimum ratio 1.5:1:2.15, flowing at a rate $\approx$ 1000 changes of gas per second, they were able to achieve single-pass gains of 28 dB/m at -60°C and of 19 dB/m at 20°C coolant temperatures. Tube voltages ranged from 4 kV to 17 kV, depending on gas pressure and temperature. The optimum tube current was 1.5 mA. Inlet pressure was in the 150-40 Torr range, and outlet pressure was in the 30-10 Torr range. The mean pressure was estimated to vary correspondingly from 100 Torr to 20 Torr.

Electron Pumping Rate

To explain how such high gain was achieved, we shall first examine the electronic pumping rate in terms of the value of E/P, the ratio of the discharge electric field to the total gas pressure.

The ionization rate ν_i is related[3] to E/P as

$$\nu_i = A\mu EP \exp[-B/(E/P)], \tag{1}$$

where A and B are constants, and μ is the electron mobility. The average electron drift velocity μE is a linear function of E/P. But ν_i is also determined by the loss rate[3] as

JSEP

$$\nu_i = \frac{D_a}{\Lambda^2}, \tag{2}$$

where D_a is the ambipolar diffusion coefficient, and Λ is related to the tube radius r_o as

$$\Lambda = \frac{r_o}{2.405}. \tag{3}$$

We attribute the loss to diffusion and neglect the effect of recombination, which is valid in view of the exceedingly small tube diameter. Equations 1 and 2 combine to show the variation of E/P with respect to pressure:

$$\left(\frac{D_a}{\Lambda^2}\right) \Big/ P \sim \frac{E}{P} \exp[-B/(E/P)]. \tag{4}$$

A small tube diameter or large D_a/Λ^2, which is the case for our capillary tube, requires a large value of E/P. Furthermore, we observe that even though E/P increases with decreasing pressure, the dependence is rather weak. A slight change of E/P in the exponent is sufficient to match any change in gas pressure. Consequently, it is reasonable to assume a constant E/P both radially and longitudinally across the tube even in the presence of a pressure gradient. This simplifies our gain computation considerably. Once we have fixed E/P, we see that N_e, the electron density, is constant along the tube. From the equation

$$J = \left[\frac{e^2 N_e}{m\nu_c}\right] E \tag{5}$$

we are able to evaluate N_e, since we know the current and discharge voltage. Here J is current density, e and m are electron charge and mass, and ν_c is the momentum transfer collision frequency which varies linearly with gas pressure P. Constant E/P implies a constant E/ν_c, and hence N_e must be constant for a fixed current density along the length of the tube. N_e has a radial Bessel function profile.

Having determined the variation of E/P and N_e throughout the tube, we may determine the electron pumping rate.[2]

The gas pressure was not the same everywhere in the tube. Actually a pressure difference of up to 100 Torr was measured between the inlet and outlet ends. We assume a uniform pressure in the tube, however, which is taken to be the average of the pressures at the inlet and outlet ends. The justification for this assumption is that it simplifies the modeling of the system, and we must be consistent in using the same mean pressure when evaluating all pressure-dependent parameters.

The E/P value at maximum gain reported was 16 V/cm-Torr. Cathode fall voltage

JSEP

was ignored in our E/P evaluation. The exact data concerning the tube voltages and their variations for different pressures and temperatures were kindly supplied by T. J. Bridges.

Theoretical Model

To predict the gain, we based our computation on the model of Allis and Haus.[2] Equations were given to allow for solving the vibrational excitation rates and also the energies of the CO_2 asymmetric and symmetric stretching modes. These equations, which were solved with the aid of a computer program written by Walter A. Stiehl, are repeated here for convenience.

$$\nu_x V_x + \nu_a V_a + \nu_b V_b = 2u_d \nu_c \tag{6}$$

$$-\xi_a \nu_x + \left(\frac{2u_d}{V_x} + \xi_a \alpha r_a\right)\nu_a = 0 \tag{7}$$

$$-\xi_b \nu_x - \xi_b r_{ax} \nu_a + \left(\frac{2u_d}{V_x}\frac{1}{1+b} + \xi_b \frac{1}{1-b} r_{bx}\right)\nu_b = 0 \tag{8}$$

$$N_e \nu_a = NC_{MN}\left(\frac{d\alpha}{dt} + \frac{\alpha - \alpha_o}{\tau_a} + \frac{C_M}{C_{MN}} R\right) \tag{9}$$

$$N_e \nu_b = 2NC_M\left(\frac{d(\sigma+\beta)}{dt} + \frac{\sigma - \sigma_o}{\tau_s} + \frac{\beta - \beta_o}{\tau_b} - R\right) \tag{10}$$

$$\frac{\sigma}{1+\sigma} = \left(\frac{\beta}{1+\beta}\right)^2. \tag{11}$$

With these six equations we solve for the six unknowns ν_x, ν_a, ν_b, α, β, and σ. The electronic level excitation rate, ν_x, is due to electron impact. The model assumes the CO_2 asymmetric stretching mode (ASM) and the N_2 vibrational mode (NVM) to be a single level. The CO_2 symmetric stretching mode (SSM) and bending mode (BM) are treated as a combined level. These two levels are characterized by vibrational temperatures T_a and T_b. The respective excitation rates by electron impact are ν_a and ν_b. u_d is the energy of a single electron in the discharge field. The momentum transfer collision frequency, ν_c, varies linearly with gas pressure P. V_x, V_a, and V_b are corresponding energies transferred at rates ν_x, ν_a, and ν_b during the inelastic collisions from the electrons to the gas molecules. Equation 6 is actually the power balance equation for a single electron. Elastic collision losses are neglected. The average quantum

JSEP

numbers of the ASM-NVM, SSM, and BM vibrational levels are α, σ, and β, which are

defined as follows.

$$\frac{a}{1+a} = \exp\left(\frac{-eV_a}{kT_a}\right) = a \tag{12}$$

$$\frac{\beta}{1+\beta} = \exp\left(\frac{-eV_b}{kT_b}\right) = b \tag{13}$$

$$\frac{\sigma}{1+\sigma} = \exp\left(\frac{-2eV_b}{kT_b}\right) = b^2, \tag{14}$$

where k is Boltzmann's constant, N the total number density of the gas mixture, C_M the CO_2 mole fraction, and C_{MN} the combined CO_2-N_2 mole fraction. R is the stimulated transition rate, $1/\tau_a$, $1/\tau_b$, and $1/\tau_s$ are the collision relaxation rates of the ASM-NVM, BM and SSM levels, respectively. Because of the known Fermi resonance between the SSM and BM levels,[4] whatever affects the SSM will also affect the BM. We assume $1/\tau_s$ to be zero so that all of the excited molecules of the SSM will leave from the BM, thereby transferring their energies, for the most part, to translational degrees of freedom. The parameters r_a, r_{ax}, and r_{bx} are previously defined constants.[2] We express ξ_a and ξ_b as

$$\xi_a = \lim_{E\to\infty} \frac{\nu_a}{\nu_c} \tag{15}$$

$$\xi_b = \lim_{E\to\infty} \frac{\nu_b}{\nu_c}. \tag{16}$$

These two parameters determine the pumping rates at high E/P: ξ_a, which reflects the excitation rate of the combined upper level, is given by

$$\xi_a = \left[\frac{C_M \nu_{eff(ASM)} + (C_{MN}-C_M)\nu_{eff(NVM)}}{C_{MN}\nu_c}\right]_{\frac{E}{P}\to\infty} \tag{17}$$

and

$$\xi_b = \left[\frac{\nu_{eff(SSM-BM)}}{\nu_c}\right]_{\frac{E}{P}\to\infty}. \tag{18}$$

The ν_{eff} are well documented by Nighan.[5]

JSEP

Average Quantum Number and the Deexcitation Rates

The model assumes that the ASM and NVM are so strongly coupled that they can be treated as a single level. The rate of vibrational energy transfer between them, measured[6] to be 1.9×10^4 sec^{-1} Torr^{-1} is huge when compared with their relaxation and excitation rates. Thus, once excited, populations of these two levels reach equilibrium quickly via the reaction

$$CO_2^* + N_2 \rightleftharpoons CO_2 + N_2^*.$$

Thereafter the combined population will remain in equilibrium while the much slower relaxation mechanisms take place. The distribution of energy from this reaction is determined by

$$\frac{da_{CO_2}}{dt} = (C_{MN}-C_M)\, KP\left[Q^* a_{N_2} - a_{CO_2}\right]$$

$$\frac{da_{N_2}}{dt} = -C_M KP\left[Q^* a_{N_2} - a_{CO_2}\right]. \tag{21}$$

Here we follow the notation of Allis and Haus[2] and define

$$NC_M a_{CO_2} + N(C_{MN}-C_M)\, a_{N_2} = NC_{MN} a, \tag{22}$$

where a_{CO_2} and a_{N_2} are the average quantum numbers of the ASM and NVM levels. K is the reaction rate of Eq. 19, and Q^* is a correction to the concentration ratio[7] that varies from 0.92 at 300°K to 0.98 at 1000°K and continues to increase to a limiting value of 1.008 at very large T. Equations 20 and 21 are obtained from Rosser et al.[7] with the much slower collision relaxation terms neglected. When solved,

$$NC_M a_{CO_2} = \frac{\psi^*}{\psi^* + 1}\, NC_{MN} a \tag{23}$$

$$N(C_{MN}-C_M)\, a_{N_2} = \frac{1}{\psi^* + 1}\, NC_{MN} a \tag{24}$$

$$\psi^* = \frac{C_M Q^*}{C_{MN} - C_M}. \tag{25}$$

JSEP

Thus, knowing the ratio of the excited CO_2 and N_2 molecules, we are able to evaluate

the relaxation rates $1/\tau_a$ and $1/\tau_b$. We assume that the excited molecules relax only through collisions and diffusion. Hence

$$\frac{1}{\tau_a} = \gamma_a + \delta \frac{D}{\Lambda^2} \tag{26}$$

$$\frac{1}{\tau_b} = \gamma_b + \delta \frac{D}{\Lambda^2}. \tag{27}$$

The γ represent the collision terms, D/Λ^2 is the diffusion rate, and δ is a constant whose value depends on the flow rate. As the flow rate increases, gradually changing from laminar to turbulent flow, both heat and mass transport rates increase. Calculations have shown that the thermal conductivity under turbulent flow is approximately twice the value under laminar flow or static condition. Hence we assign δ as 2 in Eqs. 26 and 27 for the maximum flow rate.

$$\gamma_a = \frac{\psi^*}{\psi^* + 1}\left[\frac{p_{CO_2}}{\tau_{CO_2\text{-}CO_2}} + \frac{p_{N_2}}{\tau_{CO_2\text{-}N_2}} + \frac{p_{He}}{\tau_{CO_2\text{-}He}}\right] + \frac{1}{\psi^* + 1}$$

$$\left[\frac{p_{CO_2}}{\tau_{N_2\text{-}CO_2}} + \frac{p_{N_2}}{\tau_{N_2\text{-}N_2}} + \frac{p_{He}}{\tau_{N_2\text{-}He}}\right]. \tag{28}$$

The p are partial pressures of the individual species and according to Moore et al.,[6] the $1/\tau$ are the corresponding collision rates for the $CO_2(001)$ level and the nitrogen excited level.

$$\gamma_b = \sum_m p_m k_m; \quad (m: CO_2, N_2, He) \tag{29}$$

$$\log_{10} k_m = A_m - B_m T^{-1/3}, \tag{30}$$

where T is the gas temperature, and A_m and B_m are obtained from Lyon.[8]

$$D = \frac{\psi^*}{\psi^* + 1} D_{CO_2} + \frac{1}{\psi^* + 1} D_{N_2} \tag{31}$$

$$\frac{1}{D_{CO_2}} = \frac{p_{CO_2}}{D_{CO_2\text{-}CO_2}} + \frac{p_{N_2}}{D_{CO_2\text{-}N_2}} + \frac{p_{He}}{D_{CO_2\text{-}He}} \tag{32}$$

JSEP

$$\frac{1}{D_{N_2}} = \frac{p_{CO_2}}{D_{N_2-CO_2}} + \frac{p_{N_2}}{D_{N_2-N_2}} + \frac{p_{He}}{D_{N_2-He}}. \tag{33}$$

Equations 32 and 33, including the values for the self- and binary diffusion coefficients, are given by Gordiets et al.[9] The diffusion coefficient for excited CO_2 molecules in a background gas of ground-state CO_2 molecules is different from their value which represents only the self-diffusion of ground-state CO_2 molecules. $D_{CO_2^*-CO_2}$, according to Kovacs et al.,[10] is ~35% smaller than $D_{CO_2-CO_2}$. The diffusion coefficient is also a function of gas pressure and temperature.[11]

$$D = \frac{D_o}{p}\left(\frac{T}{300}\right)^{3/2}. \tag{34}$$

Here D_o is D at 1 Torr and 300°K. The α_o, σ_o, and β_o in Eqs. 9 and 10 are simply α, σ, and β at the kinetic gas temperature T.

Gas Temperature

A high pumping rate results in a high gain if the gas does not heat up. The gain has an inverse relationship with gas temperature. The gas temperature T is normally determined by

$$Q + \frac{1}{r}\frac{d}{dr}\left(r\lambda\frac{dT}{dr}\right) = 0, \tag{35}$$

where λ is the thermal conductivity of the gas mixture, and Q is power per unit volume that is transferred to heat up the gas. The transfer of electron energy in elastic electron-atom and electron-molecule collisions is neglected[12] because it is too small to be significant. Hence we define Q as

$$Q = eN_e(\nu_a V_a + \nu_b V_b)$$

$$= J \cdot E - eN_e\nu_x V_x = 2eN_e u_d \nu_c - eN_e\nu_x V_x. \tag{36}$$

Here $eN_e\nu_x V_x$ represents the power per unit volume that is used to excite the electronic levels of the gas molecules and finally escapes by radiation, and $(\nu_a V_a + \nu_b V_b)eN_e$ is the power per unit volume transferred to the vibrational levels and eventually transferred to the gas via collision relaxations. At large E/P, $\nu_x V_x$ approaches $2u_d\nu_c$, which indicates[2] a low efficiency of the pumping mechanism for lasing. The discharge color, however, becomes brighter. Hence the fraction of input energy that goes to heating the gas actually declines for high E/P. Equation 35 can be easily solved.

JSEP

$$\int_0^{r_o} \frac{1}{r} \int_0^{r} r'Q \, dr'dr = \int_{T_w}^{T_{max}} \lambda \, dT. \tag{37}$$

It has been found[13] that over the range 300-800°K λ can be expressed within an accuracy of 1% as

$$\lambda = \lambda_o \left(\frac{T}{T_o}\right)^n, \tag{38}$$

where n depends on the gas mixture, since it is different for each individual gas component. Generally[13] it is around 0.75. The thermal conductivity at temperature T_o is λ_o, and at T_o = 273°K it was determined from the formula of Mason and Saxena.[14] Thermal conductivities and viscosities of the individual gas components that are required in the evaluation of λ_o were taken from the American Institute of Physics Handbook.[11]

Equation 35 is used generally for static or slow flow conditions. As we have already mentioned, the heat-transport mechanism is quite different when the flow rate is large. A flow is no longer laminar when the Reynolds number Re exceeds 1000. The flow is considered turbulent[15] when Re is greater than 2000.

$$\mathrm{Re} = \frac{UL}{\eta}, \tag{39}$$

where U is the velocity of the fluid, L is the characteristic length of the tube, and η is the kinematic viscosity of the fluid (see AIP Handbook). Calculation for our case showed that Re $\approx$ 1880, which implies that flow was not laminar in the experiments.

The effective heat flux q under the turbulent flow condition[16] is

$$q = (\lambda + \rho C_p \epsilon_q) \frac{\partial T}{\partial r}, \tag{40}$$

where λ is the thermal conductivity defined by Eq. 38 and ρ is the density of the gas expressed[11] as

$$\rho = \rho_o \frac{p}{760} \frac{273}{T}. \tag{41}$$

C_p is heat capacity in J/gm-deg, ϵ_q is eddy diffusivity of heat, and ϵ_q is given by Hartnett and Irvine[16] as

$$\epsilon_q = (0.124)^2 \, U(r_o - r)[1 - \exp[-(0.124)^2 \, U(r_o - r)/\eta]]. \tag{42}$$

(For ρ_o and C_p see AIP Handbook.) To simplify matters, we approximate ϵ_q as

JSEP

$$\epsilon_q = (0.124)^2 U(1/2r_o)[1 - \exp[-(0.124)^2 U(1/2r_o)/\eta]]. \quad (43)$$

Now we can define an effective thermal conductivity λ_{eff} as

$$\lambda_{eff} = \lambda + \rho C_p \epsilon_q, \quad (44)$$

and solve Eq. 37 by replacing λ with λ_{eff}. Calculations have shown that λ_{eff} is approximately two times the value of λ under static condition. T_{max} in Eq. 37 is the centerline gas temperature, and T_w is the temperature at the wall. For a conventional glass tube, T_w is ~100°K greater than the coolant temperature because of the large thermal impedance of glass.

Static Fill

The model of Allis and Haus[2] does not incorporate the effect of CO_2 dissociation and the accumulation of other chemical by-products for the static case. The influence of

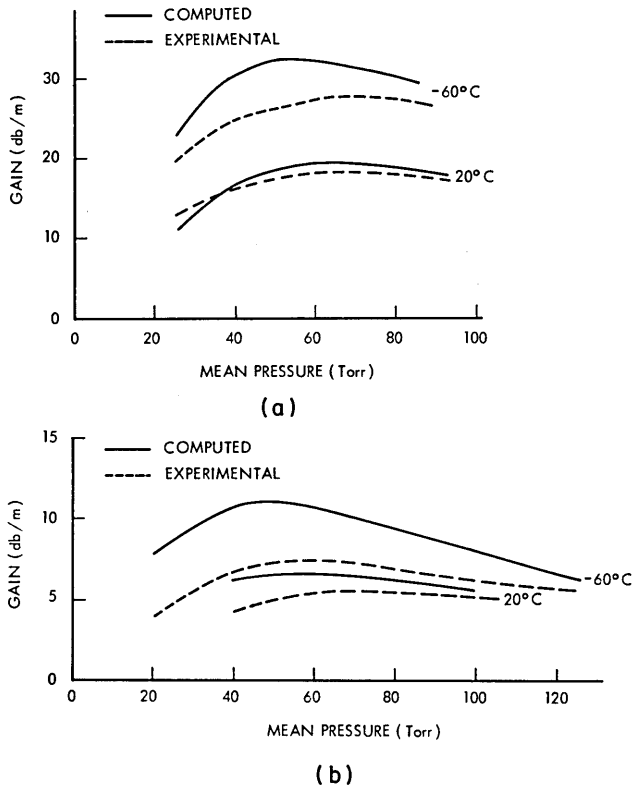

Fig. V-1. Theoretical prediction of gain vs pressure at coolant temperatures of -60°C (upper curve) and +20°C (lower curve).
(a) Flow case: rate of flow 1000 changes of gas per second.
(b) Static case.

JSEP

impurities cannot be ignored. It has been found that concentrations of neutral molecules such as CO, N, O, O_2, NO, NO_2, and of ions such as CO_3^- can be larger than electron density even for dwell time smaller than 1 millisecond.[17] The negative ion formation also plays an important role in causing plasma conditions such as ionization instability.[18] CO formation may reach 70% of the original CO_2 concentration.[19] Its presence affects the thermal conductivity of the gas mixture, that is, the upper and lower level relaxation rates, and causes changes in electron distribution and density, axial variations of the discharge field, and CO_2 concentration. The gain for the static case is from 2 to 3 times smaller[20-22] than that of the flowing case.

Figure V-1 shows our theoretical prediction of gain vs pressure at 2 different coolant temperatures for both flowing and static cases. The reported experimental results of Bridges are also shown.

Conclusion

Our study has shown to our satisfaction why the capillary tube of Bridges et al. had been able to achieve such a high gain. We found that it was due to a high electron pumping rate and a very good cooling scheme.

References

1. E. G. Burkhardt, T. J. Bridges, and P. W. Smith, Opt. Commun. 6, 193 (1972).
2. W. P. Allis and H. A. Haus, J. Appl. Phys. 45, 781 (1974).
3. S. C. Brown, Basic Data of Plasma Physics (The M. I. T. Press, Cambridge, Mass., 1967).
4. R. L. Taylor and S. Bitterman, Rev. Mod. Phys. 41, 26 (1969).
5. W. L. Nighan, Phys. Rev. A 2, 1989 (1970).
6. C. B. Moore, R. E. Wood, B-L. Hu, and J. T. Yardley, J. Chem. Phys. 46, 4222 (1967).
7. W. A. Rosser, Jr., A. D. Wood, and E. T. Gerry, J. Chem. Phys. 50, 4996 (1969).
8. D. L. Lyon, IEEE J. Quantum Electron., Vol. QE-9, No. 1, pp. 139-153, January 1973.
9. B. F. Gordiets, N. N. Sobolev, and L. A. Shelepin, Sov. Phys. – JETP 26, 1039 (1968).
10. M. Kovacs, D. R. Rao, and A. Javan, J. Chem. Phys. 48, 3339 (1968).
11. American Institute of Physics Handbook (McGraw-Hill Book Company, New York, 3rd ed., 1972), Sec. 4.
12. J. H. Waszink and J. A. J. M. Van Vliet, J. Appl. Phys. 42, 3374 (1971).
13. A. J. Laderman and S. R. Byron, J. Appl. Phys. 42, 3140 (1971).
14. E. A. Mason and S. C. Saxena, Phys. Fluids 1, 361 (1958).
15. E. R. G. Eckert, Heat and Mass Transfer (McGraw-Hill Book Company, New York, 1959).

JSEP

16. J. P. Hartnett and T. F. Irvine, Jr., Advances in Heat Transfer, Vol. 6 (Academic Press, New York, 1970), pp. 504-561.
17. W. J. Wiegand and W. L. Nighan, Appl. Phys. Letters 22, 583 (1973).
18. W. L. Nighan, W. J. Wiegand, and R. A. Haas, Appl. Phys. Letters 22, 579 (1973).
19. W. J. Wiegand, M. C. Fowler, and J. A. Benda, Appl. Phys. Letters 16, 237 (1970).
20. T. F. Deutsch, IEEE J. Quantum Electron., Vol. QE-3, No. 4, p. 151, April 1967.
21. P. K. Cheo and H. G. Cooper, IEEE J. Quantum Electron., Vol. QE-3, No. 2, p. 79, February 1967.
22. P. K. Cheo, IEEE J. Quantum Electron., Vol. QE-3, No. 12, p. 683, December 1967.

JSEP

V. QUANTUM ELECTRONICS

C. Nonlinear Phenomena

Academic and Research Staff

Prof. E. Victor George
Prof. Hermann A. Haus
Prof. Abraham Szöke
Dr. Arthur H. M. Ross

Graduate Students

Christopher P. Ausschnitt
John L. Miller

RESEARCH OBJECTIVES AND SUMMARY OF RESEARCH

JSEP

1. Laser Locking over a "Wide" Frequency Range

Joint Services Electronics Program (Contract DAAB07-74-C-0630)

Hermann A. Haus, Abraham Szöke

Intensity and frequency control of optical pulses is acquiring increased importance as these pulses are used in a variety of ways. It is especially important to provide optical pulses at a fairly high power level, and therefore we are studying the locking of a TEA laser to a stable CO_2 oscillator. This can be achieved if the natural frequency of the high-power oscillator is near that of the master oscillator.

We have previously studied the frequency characteristic of the TEA laser during a single pulse.[1,2] It was found that in the early part of the pulse the frequency varies because of the change in the refractive index of the gain medium as a consequence of the change in the population inversion as the energy is extracted from the cavity. In later stages of the pulse, the shock generated by the heating of the gas causes a much larger change in frequency. The frequency change in the early part of the pulse (~100 ns) can be minimized by proper control of the cavity length. We shall measure the cavity length using the transmission of the cavity for the stable CO_2 laser, and we shall control the length by using a slow servo.

In the first stage of the experiments the frequency chirp characteristics of the TEA laser pulse will be studied as a function of the cavity detuning. A stable CO_2 laser will be used both as a length reference and as a local oscillator (frequency reference). In this part of the study we hope that a range of cavity lengths will be found where the chirp is small.

In the second stage, the length of the cavity will be controlled by feedback, and the oscillator frequency will be controlled through the injection of a cw signal from the stable oscillator. This injection usually achieves both the control of frequency and a shortening between the time of the onset of the discharge and the laser pulse. The filter in this time delay is also reduced. All of these phenomena will be carefully evaluated.

References

1. W. A. Stiehl, "Measurement of the Spectrum of a TEA CO_2 Laser," Quarterly Progress Report No. 106, Research Laboratory of Electronics, M.I.T., July 15, 1972, pp. 63-69.

JSEP

JSEP

2. W. A. Stiehl and P. W. Hoff, "Measurement of the Spectrum of a Helical TEA CO_2 Laser," Appl. Phys. Letters 22, 680 (1973).

2. Short Laser Pulses

Joint Services Electronics Program (Contract DAAB07-74-C-0630)

U.S. Army Research Office – Durham (Contract DAHC04-72-C-0044)

Hermann A. Haus, Christopher P. Ausschnitt, Abraham Szöke

Since the crux of any system for generating ultrashort high-power optical pulses is the mode-locked oscillator, our objective is to achieve a comprehensive understanding of mode locking. In particular, we are concentrating our efforts on the saturable absorber mode locking of high-pressure CO_2 lasers.

We have developed the first closed-form theory of steady-state saturable absorber mode locking for the case of the fast relaxation time absorber[1] and also for the slow relaxation time absorber.[2] The pulses are hyperbolic secants in time. In addition, as described in Section V-C. 1, we are exploring the technique of passive mode locking with a nonlinear refractive index material. Experimental work is being carried out on high-pressure CO_2 lasers. An SF_6-He absorbing cell has been used to mode lock a pin-type TEA CO_2 laser. Pulse lengths less than 2 ns have been observed at laser pressures of half an atmosphere. We are making theoretical and experimental studies of the combined forced and passive mode locking of the TEA CO_2 laser, using a Ge acousto-optic modulator in conjunction with the absorbing cell. A high-pressure waveguide CO_2 laser is being assembled to provide a means of verifying the steady-state theory.

Future work will emphasize the development of a transient saturable absorber mode-locking theory applicable to the CO_2 TEA laser. The theory will be verified by an experimental study of the dependence of mode locking on the laser and absorber parameters. Schemes to improve the shot-to-shot reproducibility of the passive mode locking of the TEA laser will be investigated.

References

1. Hermann A. Haus, "Passive Mode-Locking Solution," Quarterly Progress Report No. 113, Research Laboratory of Electronics, M.I.T., April 15, 1974, pp. 25-29.

2. Hermann A. Haus, Christopher P. Ausschnitt, and Peter L. Hagelstein, "Slow Saturable Absorber Mode-Locking Solution," Quarterly Progress Report No. 114, Research Laboratory of Electronics, M.I.T., July 15, 1974, pp. 34-50.

JSEP

1. PASSIVE FM MODE LOCKING WITH A NONLINEAR REFRACTIVE INDEX MEDIUM

JSEP

Joint Services Electronics Program (Contract DAAB07-74-C-0630)
U.S. Army Research Office – Durham (Contract DAHC04-72-C-0044)

Christopher P. Ausschnitt, Hermann A. Haus

In a previous report[1] Professor Haus developed a theory of passive mode locking with a fast saturable absorber. The possibility of passive mode locking with a nonlinear refractive index material has been documented by others.[2, 3] The analysis presented by Laussade and Yariv,[2] however, gives no insight into the nature of the pulses that can be obtained. We shall show that the analysis of passive mode locking with a nonlinear refractive index medium parallels that of saturable absorber mode locking. Since passive mode locking induced by a nonlinear index of refraction in a medium is due to self-phase modulation, whereas with the saturable absorber it is due to self-amplitude modulation, we distinguish between the two cases by referring to them as passive FM and passive AM mode locking.

A steady-state pulse is obtained in passive FM mode locking. As in passive AM mode locking, the form of the pulse is a hyperbolic secant in time but with the distinction that there is a frequency chirp across the pulse. The pulse is unstable (saturated gain exceeds loss) if the nonlinear refractive index medium is the only mode-locking element in the cavity. We demonstrate that the pulse can be stabilized if passive FM and AM mode locking are combined.

If saturation effects are neglected, the nonlinear index of refraction has the form $n = n_o + \delta n$, where[4]

$$\tau \frac{\partial}{\partial t} \delta n = -\left(\delta n - n_2 |v(t)|^2\right), \tag{1}$$

$|v|^2$ is proportional to the instantaneous power in the incident fields, τ is the medium relaxation time, and n_2, the nonlinear coefficient, is a measure of the magnitude of the optical Kerr effect. An optical pulse traveling through such a medium is distorted in both envelope shape (self-steepening) and phase (self-phase modulation).[5] Envelope distortion can be negligible, while self-phase modulation produces large spectral broadening. Thus we neglect envelope distortion and assume that the medium thickness is much less than the self-focusing distance.

The time-variant phase shift introduced by the change in refractive index is

$$\delta\phi(t) = \frac{\omega_o}{c} \ell \, \delta n(t), \tag{2}$$

where ω_o is the center frequency of the incident pulse, ℓ is the length of the nonlinear

JSEP

JSEP

medium, and c is the free-space velocity of light. If the nonlinear medium is placed inside a laser cavity and we look for a self-consistent solution corresponding to a mode-locked pulse, the phase shift (2) seen by the cavity fields acts as a modulation of the cavity susceptance. The effect of such modulation is to generate an injection current of the form

$$I_s(t) = jG_c\, \delta\phi(t)\, v(t), \tag{3}$$

where G_c is the effective conductance or loss of the cavity. For a medium whose response is fast compared with the pulsewidth, $\tau \approx 0$ (for example, CS_2 has a $\tau = 2$ ps), (1) reduces to

$$\delta n = n_2 |v(t)|^2 \tag{4}$$

so that the injection current becomes

$$I_s = jG_c \frac{\omega_o}{c} \ell n_2 |v(t)|^2\, v(t). \tag{5}$$

For steady-state mode locking, the injection current produced by the interaction of the fields with the nonlinear medium must be balanced by the equivalent current in the laser medium and the empty cavity. In a manner directly analogous to the passive AM case,[1] we may write the mode-locking equation as

$$\left[1 + j\frac{\delta\omega_o}{\Delta\omega_c} - g\left(1 + \frac{1}{\omega_L^2}\frac{d^2}{dt^2}\right)\right] v(t) = j\frac{\omega_o}{c}\ell n_2 |v(t)|^2\, v(t), \tag{6}$$

where

$\delta\omega_o$ = uniform frequency shift of the cavity mode spectrum

$\Delta\omega_c$ = cavity mode bandwidth

g = saturated gain of the homogeneously broadened laser

ω_L = laser linewidth.

As we shall find, in contrast to the passive AM case, a frequency shift $\delta\omega_o$ of the modes is dictated by the phase modulation. In all other respects, Eq. 6 is identical to the mode-locking equation derived by Haus, with the response of the saturable absorber replaced by that of the nonlinear refractive index medium on the right-hand side.

The solution to (6) is a pulse of the form

$$v(t) = \frac{v_o}{\cosh\left(\frac{t}{\tau_p}\right)} \exp\left(j\frac{a}{\tau_p}\int^t \tanh\left(\frac{t}{\tau_p}\right) dt\right). \tag{7}$$

JSEP

The amplitude, width, and chirp parameters – v_o, τ_p and a – are constrained by the eigenvalue relations obtained by introducing (7) in (6) and balancing the terms in the hyperbolic secant and in the cube of the hyperbolic secant: JSEP

$$j\frac{\omega_o}{c}\ell n_2|v_o|^2 = \frac{g}{\omega_L^2\tau_p^2}(2 - a^2 + 3ja), \tag{8}$$

and

$$1 - g + j\frac{\delta\omega_o}{\Delta\omega_c} = \frac{g}{\omega_L^2\tau_p^2}(1 - a^2 - 2ja). \tag{9}$$

To equate the real parts of (8) we require that the chirp parameter

$$a = \sqrt{2}. \tag{10}$$

If we introduce (10) in (9), however, we find

$$1 - g = \frac{g}{\omega_L^2\tau_p^2} \tag{11}$$

in which case the saturated gain must exceed the loss in the cavity for (7) to hold. Thus the solution (7) is unstable if the nonlinear refractive index medium is the only mode-locking element in the cavity.

The addition of a saturable absorber to the cavity in conjunction with the nonlinear index of refraction medium can stabilize the pulse. For such a combined AM and FM passive mode-locking scheme, the nonlinear response term of the right-hand side of (6) becomes[1]

$$\left(\frac{Q}{Q_A^o}\frac{1}{P_A} + j\frac{\omega_o}{c}\ell n_2\right)|v(t)|^2 v(t), \tag{12}$$

where

Q = cavity quality factor

Q_A^o = absorber quality factor in the absence of power

P_A = saturation power of the absorber.

If a solution of the form of (7) is assumed, (8) becomes JSEP

JSEP

$$\left(\frac{Q}{Q_A^o}\frac{1}{P_A} + j\frac{\omega_o}{c}\ell n_2\right)|v_o|^2 = \frac{g}{\omega_L^2\tau_p^2}(2 - a^2 + 3ja). \tag{13}$$

Because the left-hand side now has a positive real part because of the absorber, a can assume values $a^2 < 2$. Furthermore, from (9) we see that the stability of the solution requires that

$$a^2 < 1. \tag{14}$$

Equations (9) and (13) are supplemented by the dependence of the laser gain upon the power P

$$g = \frac{g_o}{1 + \frac{P}{P_L}}, \tag{15}$$

where g_o is the small-signal gain, and P_L is the saturation power of the laser medium. If we assume a pulse repetition rate T, the average power is also related to the pulse parameters by

$$P = \frac{1}{T}\int_{-\infty}^{\infty}\left|\frac{v_o}{\cosh\left(\frac{t}{\tau_p}\right)}\right|^2 dt = \frac{2\tau_p}{T}|v_o|^2. \tag{16}$$

The simultaneous solution of (9), (13), and (15) completely specifies the system and pulse parameters g, $\delta\omega_o$, a, τ_p, and P. Stable solutions will exist if the conditions are such that (14) holds.

We have shown that passive FM mode locking alone does not lead to stable solutions. Thus the pulses observed by Comly et al.,[3] if stable, could not have been due solely to the influence of the index of refraction nonlinearity in the cavity. Combined AM and FM passive mode-locking, however, does give stable pulse solutions of the form (7). Such pulses are of interest because of their frequency chirp which facilitates subsequent pulse compression.

References

1. H. A. Haus, "Mode Locking with a Fast Saturable Absorber" (to be submitted for publication); "Short Laser Pulses: Passive Mode-Locking Solution," Quarterly Progress Report No. 113, Research Laboratory of Electronics, M. I. T., April 15, 1974, pp. 25-29.

2. J. Laussade and A. Yariv, IEEE J. Quantum Electron., Vol. QE-5, No. 9, p. 435, September 1969.

JSEP

3. J. Comly, E. Garmire, J. P. Laussade, and A. Yariv, Appl. Phys. Letters 13, 176 (1968). JSEP
4. J. Frenkel, Kinetic Theory of Liquids (Dover Publications, Inc., New York, 1955).
5. F. DeMartini, C. H. Townes, T. K. Gustafson, and P. L. Kelley, Phys. Rev. 164, 312 (1967). JSEP